

Painted turtle cortex is resistant to an *in vitro* mimic of the ischemic mammalian penumbra

Matthew Edward Pamerter^{1,6}, David William Hogg^{2,6}, Xiang Qun Gu¹,
Leslie Thomas Buck^{2,3} and Gabriel George Haddad^{1,4,5}

¹Division of Respiratory Medicine, Department of Pediatrics, University of California San Diego, La Jolla, California, USA; ²Department of Cell and Systems Biology, University of Toronto, Toronto, Ontario, Canada; ³Department of Ecology and Evolutionary Biology, University of Toronto, Toronto, Ontario, Canada; ⁴Department of Neurosciences, University of California San Diego, La Jolla, California, USA; ⁵The Rady Children's Hospital-San Diego, San Diego, California, USA

Anoxia or ischemia causes hyperexcitability and cell death in mammalian neurons. Conversely, in painted turtle brain anoxia increases γ -amino butyric acid (GABA)ergic suppression of spontaneous electrical activity, and cell death is prevented. To examine ischemia tolerance in turtle neurons, we treated cortical sheets with an *in vitro* mimic of the penumbral region of stroke-afflicted mammalian brain (ischemic solution, IS). We found that during IS perfusion, neuronal membrane potential (V_m) and the GABA_A receptor reversal potential depolarized to a similar steady state (-92 ± 2 to -28 ± 3 mV, and -75 ± 1 to -35 ± 3 mV, respectively), and whole-cell conductance (G_w) increased >3-fold (from 4 ± 0.2 to 15 ± 1 nS). These neurons were electrically quiet and changes reversed after reperfusion. GABA receptor antagonism prevented the IS-mediated increase in G_w and neurons exhibited enhanced electrical excitability and rapid and irreversible rundown of V_m during reperfusion. These results suggest that inhibitory GABAergic mechanisms also suppress electrical activity in ischemic cortex. Indeed, after 4 hours of IS treatment neurons did not exhibit any apparent damage; while at 24 hours, only early indicators of apoptosis were present. We conclude that anoxia-tolerant turtle neurons are tolerant of exposure to a mammalian ischemic penumbral mimic solution.

Journal of Cerebral Blood Flow & Metabolism (2012) 32, 2033–2043; doi:10.1038/jcbfm.2012.103; published online 18 July 2012

Keywords: anoxia tolerance; anoxic depolarization; apoptosis; electrophysiology; GABA; spike arrest

Introduction

Most vertebrates suffer brain damage within minutes of anoxia; however, facultative anaerobes such as the Western painted turtle, *Chrysemys picta belli*, survive anoxia for days to months without apparent injury (Bickler and Buck, 2007). The key to this tolerance is the maintenance of ATP supply via a coordinated reduction of ATP demand in the absence of oxygen (Bickler and Buck, 2007). In mammals,

50% to 60% of total brain ATP consumption is attributable to Na⁺/K⁺-ATPase-mediated ion pumping to maintain ionic gradients and synaptic activity (Erecinska and Silver, 1989; Hansen, 1985); while at the cellular level, action potential (AP) generation and propagation, and excitatory postsynaptic potentials account for ~81% of neuronal energy expenditure (Attwell and Laughlin, 2001). Therefore, limiting excitatory electrical activity is key to tolerating prolonged low-oxygen stress. Facultative anaerobes defend ATP supplies during anoxia by reducing the workload on ATPases through the mechanisms of 'channel arrest' and 'spike arrest' (Feng *et al*, 1988; Hochachka, 1986), which reduce ion leakage and neuronal excitability.

Channel arrest is a mechanism whereby membranes become less permeant to ions during anoxia, thereby reducing the requirement for compensatory ion-motive ATPase activity. In anoxic turtle brain, the conductance and expression of ion channels, in particular excitatory glutamatergic receptors, are rapidly and reversibly decreased (Bickler *et al*, 2000; Pamerter *et al*, 2008), thereby reducing ionic flux and

Correspondence: Dr ME Pamerter, Department of Pediatrics, University of California San Diego, 9500 Gilman Dr, La Jolla, CA 92093-0735, USA.

E-mail: mpamerter@ucsd.edu

⁶These authors contributed equally to this work.

This work was supported in part by the National Institutes of Health (5P01HD032573 to GGH, P30 NS047101 to the UCSD Neurosciences Microscopy Shared Facility); a Natural Sciences and Engineering Research Council of Canada Discovery grant to LTB; a Heart and Stroke Foundation of Canada PDF to MEP; and an Ontario Graduate Scholarship to DWH.

Received 10 May 2012; revised 15 June 2012; accepted 19 June 2012; published online 18 July 2012

opposing excitatory depolarization. Concomitantly, γ -amino butyric acid (GABA), the primary inhibitory neurotransmitter in adult mammalian central nervous system (Krnjevic, 1997), increases >80-fold in anoxic turtle brain (Nilsson and Lutz, 1991), which activates a dominant conductance to Cl^- ions, clamping neuronal membrane potential (V_m) near the Cl^- ion reversal potential (E_{Cl} or E_{GABA}) and opposing excitatory depolarization via a shunt-like inhibitory mechanism (i.e., spike arrest; Pamerter *et al*, 2011). Together, these neuroprotective mechanisms act to decrease neuronal excitability, ionic flux, and compensatory ion pump activity, thus preserving ATP and enabling neuronal survival during prolonged anoxia (Buck *et al*, 1998; Hylland *et al*, 1997; Pamerter and Buck, 2008; Pamerter *et al*, 2011).

Based on these adaptations, *C. picta* has been championed as a model of anoxia tolerance in which to explore protective mechanisms against low-oxygen insult in brain (Bickler and Buck, 2007). However, in mammalian ischemic stroke pathologic examination, the deleterious effects of anoxia or hypoxia are compounded by impaired cerebral blood flow, which also limits nutrient delivery and slows the removal of signaling molecules, ions, and metabolically derived lactate and CO_2 (Branston *et al*, 1974). These events enhance cytotoxicity, ionic imbalance, and acute acidification in the occluded region (the infarct core) and hypoperfused surrounding tissue (the penumbra) (Anderson *et al*, 1999; Yao *et al*, 2007). Similarly to the mammalian ischemic penumbra, turtle brain pH becomes more acidic during anoxia (Buck *et al*, 1998; Wasser *et al*, 1991); however, cerebral blood flow is increased (Bickler, 1992) and liver glycogen stores are mobilized and continuously delivered to the brain, facilitating glycolytic ATP production (Bickler and Buck, 2007). This represents a significant systemic advantage relative to ischemic stress in mammals; however, turtles are also considerably more tolerant to ischemic stress and survive >1 hour after cardiac excision at 22°C (Belkin, 1968). Furthermore, mimicking the turtle's endogenous cell-level neuroprotective mechanisms (inhibiting glutamatergic activity—channel arrest, or enhancing GABAergic activity—spike arrest) is neuroprotective against ischemic or hypoxic injury in mammalian brain (Arundine and Tymianski, 2004; Costa *et al*, 2004). Therefore, the ability of anoxia-tolerant turtle brain to withstand ischemic stress is of interest to better understand how neuroprotective adaptations to low-oxygen environments may provide protection against more complex ischemic challenges.

Previous attempts to examine the resistance of anoxia-tolerant turtle neurons to ischemic stress have relied on oxygen-glucose deprivation or chemical mimics of ischemia that model the mammalian infarct core (i.e., iodoacetate and sodium cyanide to inhibit glycolysis and oxidative phosphorylation, respectively, e.g., Doll *et al*, 1991), where cell death occurs within minutes of insult onset. Conversely,

the penumbral region is hypoperfused and therefore hypoxic, and cell death here spreads over hours to days postinsult and accounts for the majority of morbidity and mortality after stroke in mammalian models (Lo, 2008). Therefore, mechanisms of neuroprotection in this region are of considerably greater clinical relevance than in the infarct core. Recently, our laboratory developed an *in vitro* treatment paradigm that mimics the key ionic, hypoxic, and acidic parameters of the penumbral milieu, termed as ischemic solution (IS; Yao *et al*, 2007), and we asked whether anoxia-tolerant turtle cortical neurons are resistant to this clinically relevant ischemic stress. To answer this question, we examined ischemia tolerance in pyramidal neurons from intact cortical sheets because synaptic connectivity and endogenous neurotransmitter release are maintained in this preparation *ex vivo* (Blanton *et al*, 1989; Feng *et al*, 1988). Specifically, we treated turtle cortical sheets with artificial cerebral spinal fluid (ACSF) or IS for up to 24 hours, and examined pyramidal neuron viability and synaptic activity using the whole-cell and perforated-patch electrophysiological techniques and also molecular and biochemical viability assays.

Materials and methods

Please see Supplementary information for an expanded description of Materials and methods.

This study was approved by the University of California San Diego Institutional Animal Care and Use Committee and the University of Toronto Animal Care Committee. Cortical slice dissection and patch-clamp recording methods are described elsewhere (Pamerter *et al*, 2011). Briefly, cortical sheets were dissected and placed in a bath with flow-through perfusion system. Neurons were perfused with (1) ACSF (in mmol/L: K^+ 2.6, Na^+ 107, Cl^- 113, Ca^{2+} 1.2, Mg^{2+} 1.0, NaH_2PO_4 2.0, NaHCO_3 26.5, glucose 10, imidazole 5 (280 to 290 mOsm, pH 7.4, 21% O_2 , 5% CO_2 , balance N_2); Pamerter *et al*, 2011) at 4°C, (2) ACSF at 24°C, or (3) an ischemic penumbral perfusate mimic (IS, in mmol/L: K^+ 64, Na^+ 51, Cl^- 77.5, Ca^{2+} 0.13, Mg^{2+} 1.5, glucose 3.0, glutamate 0.1 (315 mOsm, pH 6.5, 1.5% O_2 , 15% CO_2 , balance N_2); Yao *et al*, 2007) at 24°C; alone or with pharmacological modifiers as specified in Results section. In some experiments, cortical sheets were treated with ACSF containing high $[\text{K}^+]$ or with IS containing normal $[\text{K}^+]$ (2.6 mmol/L). Electrical activity was recorded for up to 2 hours from pyramidal neurons using an Axon multiclamp 700B amplifier and Clampex 10 software (Molecular Devices, Sunnyvale, CA, USA). For perforated-patch experiments, electrodes were back-filled with intracellular cerebral spinal fluid containing 25 $\mu\text{g}/\text{mL}$ gramicidin.

Cell viability was assessed using propidium iodide (PI) exclusion, annexin V expression, DNA 'comet-tail', and ATP-luciferase assays. The PI and annexin V fluorescence were examined using an Olympus FV1000 scanning confocal microscope, with 572 nm (TRITC) and 488 nm (FITC) laser lines (Olympus, San Diego, CA, USA).

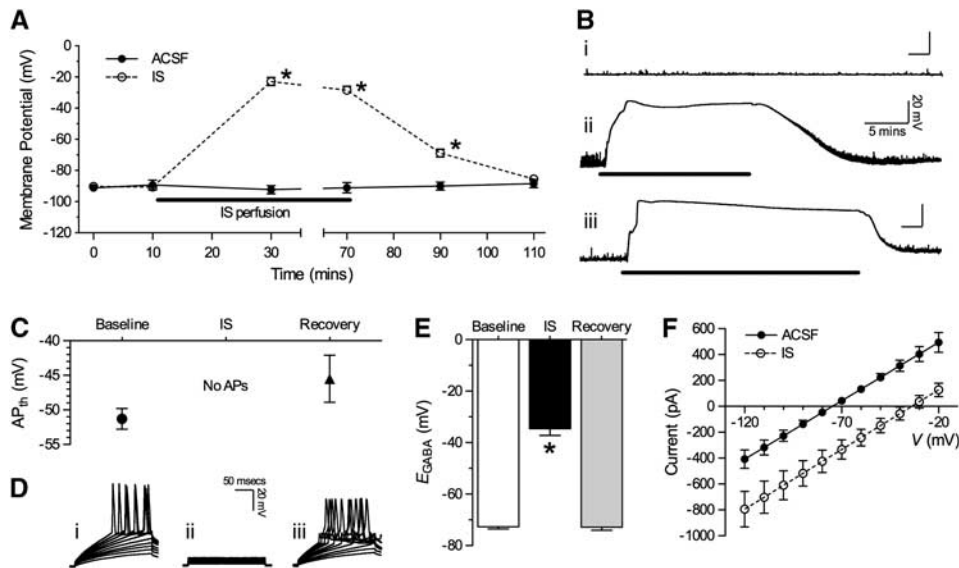


Figure 1 IS-treated cortical neuronal membrane potential (V_m) depolarizes to E_{GABA} . **(A)** Summary of V_m recordings from cortical neurons treated with ACSF or IS for 110 minutes. **(B)** Sample V_m recordings from patch-clamped neurons treated with (i) ACSF or (ii) 20 or (iii) 60 minutes IS perfusion with recovery. Black bars indicate duration of IS perfusion. **(C)** Summary of action potential (AP) threshold (AP_{th}) from stimulated neurons treated as indicated. APs could not be elicited during IS treatment. **(D)** Sample recordings of evoked APs recorded during baseline control (i), IS perfusion (ii), and normoxic reperfusion (iii). **(E)** Summary of GABA_A receptor reversal potentials (E_{GABA}). **(F)** Summary I/V curves of E_{GABA} in ACSF (solid line) and IS (dashed line) from **(E)**. Data are mean \pm s.e.m. Asterisks (*) indicate significant difference from normoxic controls. V_m data are from 10 to 26 separate experiments for each treatment, E_{GABA} data are averaged recordings from 12 separate neurons. Treatments: artificial cerebral spinal fluid (ACSF) and ischemic solution (IS). GABA, γ -amino butyric acid.

Statistical Analysis

Data were analyzed using a two-tailed Student's t -test or one-way analysis of variance, followed by Dunnett's post test. Significances were indicated if $P < 0.05$ assuming two groups had an equal variance.

Results

Cortical Neurons Are Reversibly Depolarized During Ischemic Solution Perfusion

In normoxia, neurons exhibited a steady resting membrane potential (V_m) of -90.3 ± 1.1 mV in recordings of up to 2 hours ($n = 10$, Figures 1A and 1B(i)), and voltage ramps elicited APs at a threshold (AP_{th}) of -51.3 ± 1.0 mV (Figures 1C and 1D), values which are similar to previous measurements from normoxic turtle cortex (Pamerter *et al*, 2011). Conversely, upon IS perfusion neurons rapidly depolarized ~ 60 to 70 mV to a new steady state ($V_m = -22.9 \pm 1.35$ mV after 20 minutes and -28.4 ± 2.3 mV after 60 minutes IS perfusion, respectively; $n = 26$, Figures 1A and 1B(ii, iii)). Notably, neurons did not exhibit excitatory events during the initial depolarization and were electrically quiet during the entire period of IS treatment, such that APs could not be evoked ($n = 26$, Figures 1C and 1D). These changes were reversed by IS washout with normoxic ACSF. V_m hyperpolarized to -68.6 ± 9.3 mV after 20 minutes

reperfusion, and at 40 minutes was not significantly different from pre-IS baseline controls (-85.4 ± 1.5 mV). Neuronal excitability also returned after reperfusion, as evidenced by the firing of APs in response to stimuli (recovery $AP_{th} = -45.5 \pm 3.4$ mV, Figures 1C and 1D).

In ischemic mammal brain, neuronal depolarization is deleterious and leads to seizure-like events and irreversible anoxic depolarization within minutes of insult onset; and therefore, the lack of similar electrical hyperexcitation in IS-treated turtle neurons, despite a rapid and marked V_m depolarization, suggests that inhibitory (i.e., spike arrest) mechanisms are strongly recruited during IS treatment and reperfusion in this model. In anoxic turtle neurons, V_m is 'clamped' at E_{GABA} , which is determined by the distribution of Cl^- across the plasma membrane (E_{Cl}); however, the IS used in our experiments incorporates deleterious ionic imbalances that are characteristic of the penumbral milieu, which would alter this distribution. Therefore, to assess a potential role in the IS-mediated depolarization of V_m , we measured E_{GABA} to determine the new set point of Cl^- distribution during IS. In normoxia, E_{GABA} was -72.7 ± 0.8 mV and depolarized relative to control V_m ($n = 20$, Figures 1E and 1F); whereas during IS perfusion E_{GABA} depolarized to -31.6 ± 2.6 mV and was not significantly different from V_m in IS at the same time point. After normoxic reperfusion, E_{GABA} returned to baseline levels (-72.9 ± 1.2 mV). This depolarization

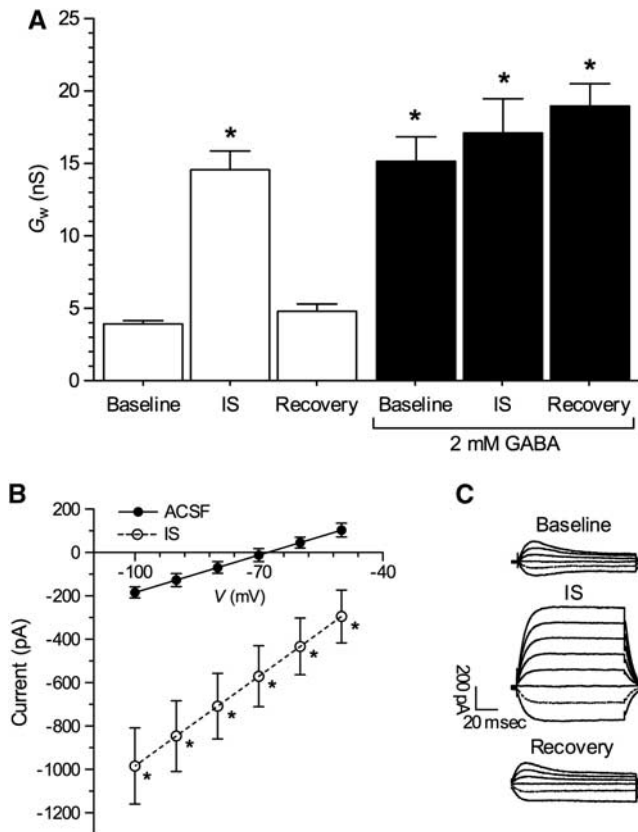


Figure 2 Ischemic solution (IS) and γ -amino butyric acid (GABA) increase whole-cell conductance (G_w). **(A)** Summary of G_w recordings from cortical neurons treated with artificial cerebral spinal fluid (ACSF) or IS alone (white bars) or cotreated with GABA (black bars). **(B)** Summary I/V curves of G_w in ACSF (solid line) and IS (dashed line) from **(A)**. **(C)** Sample raw G_w voltage-clamp recordings from **(A)**. Data are mean \pm s.e.m. Asterisks (*) indicate significant difference from normoxic controls. Data are from 25 to 31 separate experiments for each treatment, I/V curves are averaged recordings from 10 separate neurons. Treatment as per Figure 1, and 2 mmol/L GABA.

represents a significant increase in intercellular chloride ($[Cl^-]_i$). According to the Nernst potential equation $[Cl^-]_i$ in ACSF is ~ 6.3 mmol/L (extracellular chloride ($[Cl^-]_o$) = 113 mmol/L), whereas after the transition to IS, $[Cl^-]_i$ increases to ~ 22.2 mmol/L ($[Cl^-]_o$ = 77.5 mmol/L).

Neuronal Membrane Conductance is Greatly Increased During Ischemic Solution Treatment

Spike arrest in turtle cortical neurons is mediated by an increase in GABA-sensitive Cl^- conductance (G_{Cl}), which resets V_m to E_{GABA} (Pamenter *et al*, 2011). Therefore, since neuronal V_m and E_{GABA} depolarized to similar levels (approximately -30 mV) during IS perfusion but neurons did not exhibit electrical excitation we hypothesized that a similar increase in G_{Cl} occurs during ischemia, and that this increase underlies the depolarization of V_m to E_{GABA} . To test this hypothesis, we examined

changes in whole-cell conductance (G_w) during IS perfusion. At rest, neuronal G_w was 3.9 ± 0.2 nS, but increased >3 -fold to 14.6 ± 1.3 nS during IS perfusion ($n = 31$, Figures 2A to 2C); and G_w recovered to pre-IS control levels on reperfusion (4.8 ± 0.5 nS). We have previously shown that 2 mmol/L GABA administration induces similar-magnitude changes to G_w in turtle neurons (Pamenter *et al*, 2011); therefore, in separate experiments we treated cortical sheets with GABA during an ACSF to IS transition with recovery. In these experiments, G_w in neurons pretreated for 15 seconds with 2 mmol/L GABA was 15.1 ± 1.7 nS in normoxic ACSF and 17.1 ± 2.4 nS in IS ($n = 14$, Figure 2A). These conductance states were not significantly different from GABA-free IS-treated samples.

Next, we examined the effect of preventing the inhibitory action of spike arrest mechanisms during IS perfusion by blocking GABA_A and GABA_B receptors with picrotoxin or gabazine (GZ), and CGP55845 (CGP), respectively, because we have previously shown that both GABA receptor subtypes contribute to spike arrest mechanisms in anoxic turtle cortex (Pamenter *et al*, 2011). In these experiments, neurons exhibited electrical excitability during the transition to IS perfusion ($n = 5$, Figure 3A, segment a) and also after normoxic reperfusion (Figure 3A, segment b). In all experiments, V_m was more depolarized during IS perfusion with GABA blockers than with IS alone (-15.7 ± 0.6 versus -28.4 ± 2.3 mV, Figure 3B); and after normoxic reperfusion increased spontaneous APs were observed and V_m did not recover, whereas in neurons treated with IS alone V_m returned to baseline levels (-19.4 ± 1.5 and -82.0 ± 2.0 mV after 30 minutes reperfusion, respectively; Figures 3A and 3B). Importantly, the IS-mediated increase in G_w was prevented by GABA receptor antagonism (G_w was 4.5 ± 0.8 and 6.3 ± 1.5 nS before, and during IS + GZ + CGP perfusion, respectively, Figures 3C and 3D).

High External $[K^+]$ Increases GABAergic Inhibitory Tone

Neuronal membrane potential is determined primarily by the K^+ gradient (Hodgkin and Huxley, 1952). Similarly, E_{GABA} is largely determined by this gradient through the activity of K^+/Cl^- cotransporters, such that increases in extracellular $[K^+]$ are expected to depolarize E_{GABA} (Rivera *et al*, 1999; Thompson and Gahwiler, 1989). External $[Cl^-]$ is reduced from 113 to 77.5 mmol/L in IS relative to ACSF, which would account for an ~ 10 mV depolarizing shift in E_{GABA} (Nernst potential equation); however during IS perfusion, E_{GABA} was much more depolarized (by ~ 30 to 40 mV), indicating that the internal $[Cl^-]$ is altered by IS perfusion in addition to changes to external $[Cl^-]$. Since K^+ is greatly increased in the mammalian ischemic penumbra and in our penumbral mimic solution, we next examined the impact of altered K^+ on neuronal

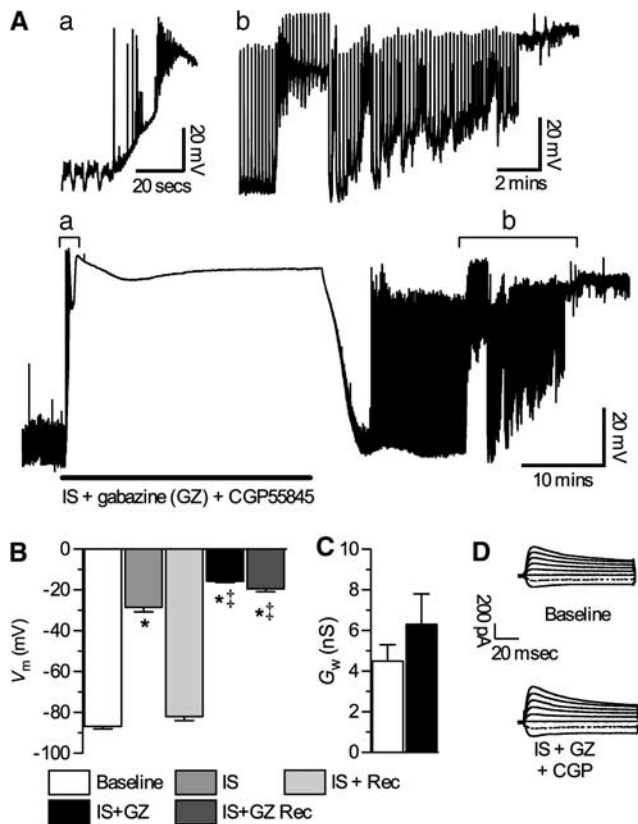


Figure 3 GABA receptor antagonism during ischemic solution (IS) causes electrical hyperexcitation and V_m depolarization after normoxic reperfusion. (A) Sample V_m recording from a patch-clamped neuron cotreated with IS plus the GABA_A receptor antagonist gabazine (GZ) and the GABA_B receptor antagonist CGP55645 (CGP). Insets (a and b) are enlargements of the corresponding time period on the full trace (below). Black bar indicates duration of IS plus GZ and CGP treatment. (B) Summary of V_m changes from (A). (C) Summary of G_w changes from cells in (A). (D) Sample raw G_w voltage-clamp recordings from (C). Data are mean ± s.e.m. from five separate experiments. Asterisks (*) indicate significant difference from control treatment and double daggers (‡) indicate significant difference from IS alone. Treatment as per Figure 1, and 25 μmol/L GZ and 5 μmol CGP. GABA, γ-amino butyric acid.

electrical activity and GABAergic inhibition in normoxia and during IS treatment in turtle brain. First, we treated cortical sheets with a high-K⁺ ACSF solution containing 64 mmol/L K⁺ (to match the K⁺ composition of IS). In these experiments, neurons rapidly depolarized ~75 mV and V_m was -10.3 ± 2.3 mV after 30 minutes perfusion ($n=9$, Figures 4A and 4B). E_{GABA} was similarly depolarized by high-K⁺ ACSF to -44.6 ± 2.2 mV ($n=5$, raw data not shown), neurons were electrically quiet during this depolarization (Table 1), and V_m returned to baseline levels after 30 minutes reperfusion with normal ACSF. Similarly, G_w reversibly increased from 4.6 ± 0.7 to 12.3 ± 1.5 nS when neurons were treated with high-K⁺ ACSF ($n=5$, Figures 4C and 4D), a conductance state that is consistent with that of normoxic neurons during GABA application.

To examine the role of GABA in high-K⁺-mediated changes, we next applied 2 mmol/L GABA during an ACSF to high-K⁺ ACSF transition with recovery. In this analysis, GABA-treated neurons were slightly depolarized with regard to untreated neurons (-78.6 ± 2.5 mV, $n=5$, Figure 4B), and reversibly depolarized to -20.0 ± 2.3 mV after 30 minutes perfusion of high-K⁺ ACSF with GABA application. G_w was increased by GABA treatment alone (13.3 ± 2.3 nS, $n=5$ for each, Figures 4C and 4D) and the subsequent switch to high-K⁺ ACSF with GABA had no additional effects on G_w (13.0 ± 2.3 nS). In addition, APs could not be evoked from neurons treated with high-K⁺ ACSF alone or in the presence of GABA ($n=9$ and 5, respectively, Table 1). Taken together, these results indicate that inhibitory GABAergic activation (i.e., GABA release), and the depolarizing shift in E_{GABA} occurs downstream of elevated extracellular K⁺ accumulation since GABA perfusion alone increases G_w but does not markedly depolarize neurons, whereas high-K⁺ ACSF perfusion alone increases G_w to the same degree as GABA perfusion and also depolarizes neurons, while simultaneously preventing electrical excitability.

This relationship was indirectly confirmed in experiments examining the effect of a modified IS perfusate containing low [K⁺] (2.6 mmol/L). In these experiments, neurons treated with low-K⁺ IS did not exhibit significant depolarization of V_m , G_w did not increase, and potentials could be evoked with stimulus injection ($n=8$, Figures 4A to 4D, Table 1). In addition, E_{GABA} was not depolarized relative to controls ($n=5$, -75.0 ± 0.6 mV, raw data not shown). Conversely, application of GABA in low-K⁺ IS restored the large increase in G_w observed in control IS experiments and ablated stimulus-evoked potentials, but did not restore the depolarization of V_m , indicating that E_{GABA} was not markedly depolarized by low-K⁺ IS perfusion. Therefore, increased GABA release and postsynaptic G_w , along with the IS-mediated shift in E_{GABA} , are regulated by high-K⁺ in the unmodified IS perfusate such that the change in V_m and electrical inhibition is due to increased presynaptic release of GABA, while the change in E_{GABA} is due to postsynaptic alterations of neuronal K⁺ gradients with a smaller contribution from a reduced driving force on Cl⁻ due to lower [Cl⁻]_o.

Turtle Neurons Tolerate Prolonged Ischemic Solution Treatment

Finally, we examined the ability of turtle cortical sheets to survive prolonged IS treatment. It is not feasible to assay long-term cell viability using electrophysiological approaches; therefore, we used a variety of biochemical and molecular assays to examine the effects of prolonged IS perfusion (0.5 to 24 hours) on turtle cortical sheet viability. Necrotic cell death is generally characterized by rapid permeability barrier (plasma membrane) rupture in the absence of apoptotic

markers (Galluzzi *et al*, 2007); therefore, we first examined membrane viability using a PI exclusion assay in live cortical sheets bathed in ACSF or IS treated at 24°C ($n=3$ for each, Figure 5A). The PI fluorescence was assessed at 0.5, 1, 2, 4, 8, 12, and 24 hours, and at each of these time points PI fluorescence was unchanged in either treatment group relative to controls treated in ACSF at 4°C. In other experiments, PI fluorescence was assessed in combination with the translocation of the apoptotic marker annexin V to the outside of neuronal plasma membranes. After 4 hours of IS treatment, we did not observe significant PI or annexin V fluorescence in either ACSF or IS perfused cortical sheets treated at 24°C relative to controls treated with ACSF at 4°C ($n=5$ for each, Figures 5B and 5C). Similarly, after

24 hours treatment neurons in all groups continued to exclude PI; however, the extent of annexin V fluorescence in IS-treated samples increased ~6-fold relative to controls, indicating the occurrence of apoptosis in IS-treated cortical sheets. In parallel experiments, cortical sheets were treated with the proapoptotic agent staurosporine in ACSF. Relative to controls staurosporine increased annexin V fluorescence ~11- and 15-fold at 4 and 24 hours, respectively ($n=3$, Figures 5B and 5C).

To further examine cell viability at 24 hours, we examined DNA fragmentation using a DNA gel electrophoresis assay, since ladderized oligonucleosomal DNA fragmentation is a hallmark of advanced apoptosis (Galluzzi *et al*, 2007). In this analysis, we did not observe fragmentation in ACSF- or IS-treated

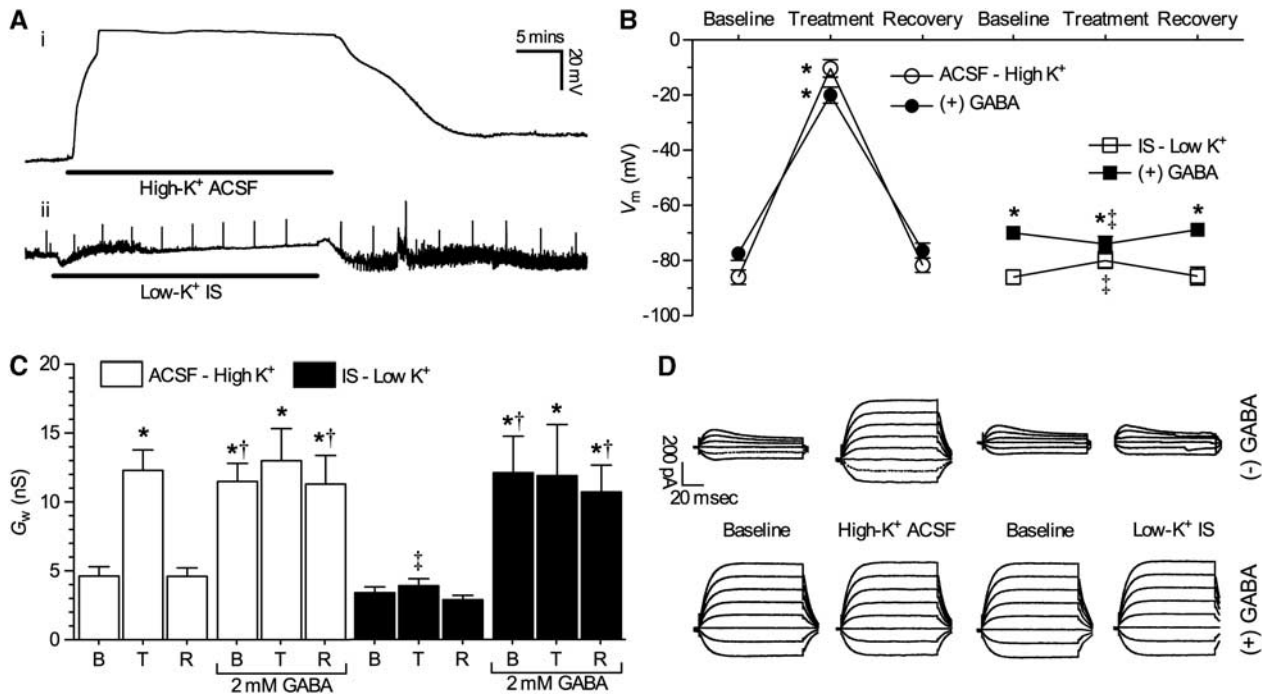


Figure 4 Extracellular K^+ underlies the ischemic solution (IS)-mediated V_m depolarization and increase in G_w . **(A)** Sample V_m recordings from patch-clamped neurons treated with (i) high- K^+ artificial cerebral spinal fluid (ACSF) or (ii) low- K^+ IS, and after 30 minutes recovery. Black bars indicate duration of treatment perfusion. **(B)** Summary of V_m recordings from cortical neurons treated as indicated. **(C)** Summary of G_w changes from cells in **(A)**. **(D)** Sample raw G_w voltage-clamp recordings from **(C)**. Data are mean \pm s.e.m. from 5 to 9 separate experiments. Asterisks (*) indicate significant difference from normoxic controls; daggers (†) indicate significant difference from normoxia at the same time point; and double daggers (‡) indicate significant difference from IS alone. Treatment as per Figure 2 and ACSF with high- K^+ (64 mmol/L), and IS with low- K^+ (2.6 mmol/L). GABA, γ -amino butyric acid.

Figure 5 Ischemic solution (IS) perfused cortical sheets retain DNA and plasma membrane integrity, but express an early apoptotic marker at 24 hours. **(A)** Summary of fold change of propidium iodide (PI) fluorescence imaged from live cortical sheets treated at 24°C relative to PI fluorescence in control samples treated simultaneously with artificial cerebral spinal fluid (ACSF) at 4°C. **(B)** Summary of fold change of apoptotic annexin V fluorescence. **(C)** Overlay sample images from **(B)** of PI (red) and annexin V (green) fluorescence in cortical sheets treated as indicated. **(D)** Gel image of oligonucleosomal DNA fragment separation via electrophoresis on a 1.5% conventional agarose gel. **(E)** Summary of [ATP] from cortical sheets treated as indicated. Data are mean \pm s.e.m. from 3 to 5 separate experiments for each treatment. Asterisks (*) indicate significant difference from control treatment; daggers (†) indicate significant difference from normoxia at the same time point; and double daggers (‡) indicate significant difference from IS alone. Treatment as per Figure 1, and 5 μ mol/L staurosporine (STS), control in ACSF at 4°C, and 24 hours IS plus 1-hour recovery. The color reproduction of this figure is available at the *Journal of Cerebral Blood Flow and Metabolism* journal online.

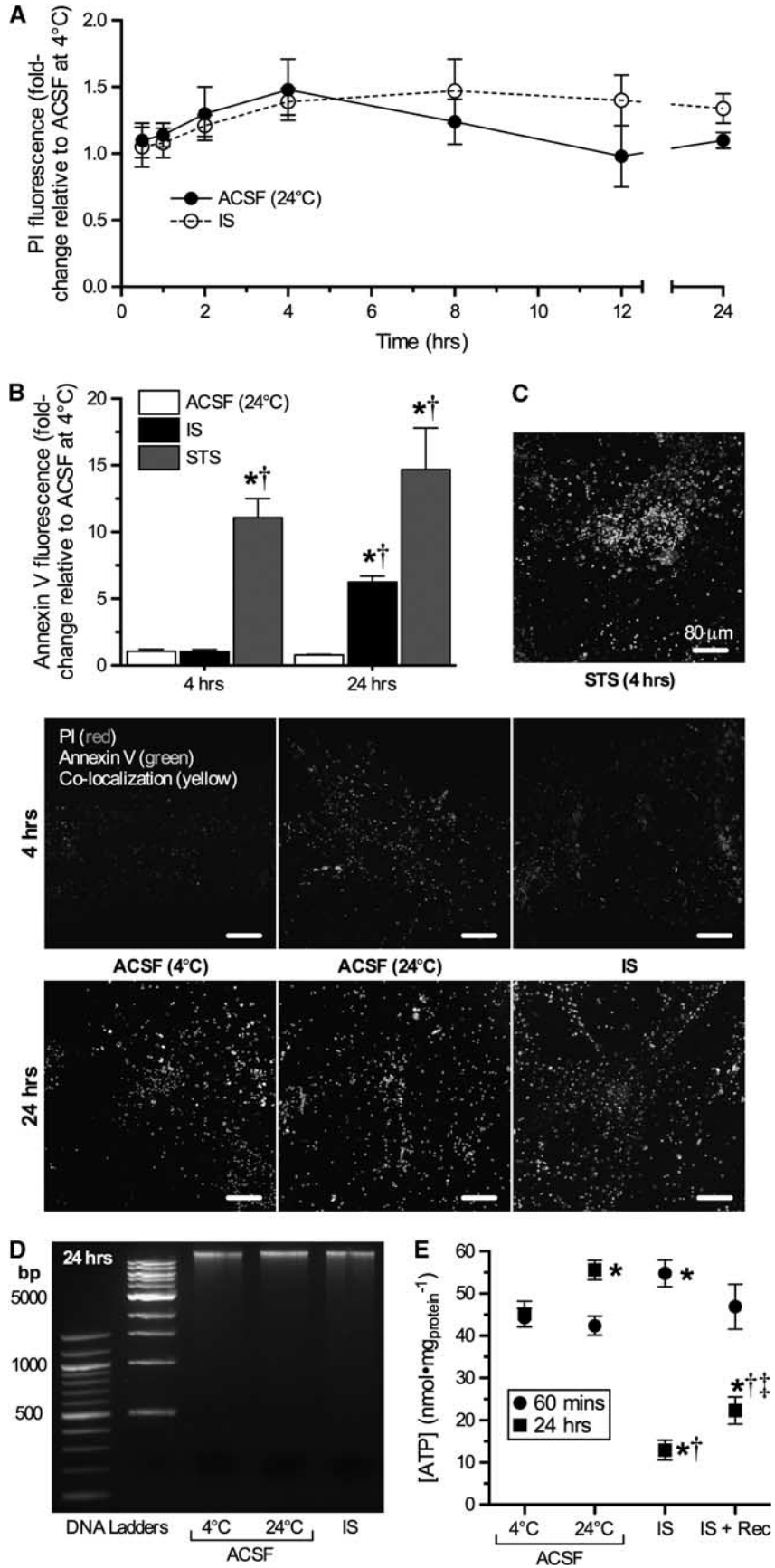


Table 1 Effects of extracellular $[K^+]$ and GABA on AP_{th}

Experimental condition	AP_{th} (mV)		
	Baseline	Treatment	Recovery
High- K^+ ACSF	-48.4 ± 1.2 (9)	No APs (9)*	-46.1 ± 1.7 (9)
High- K^+ ACSF w/GABA	No APs (5)*†	No APs (5)*	No APs (5)*†
Low- K^+ IS	-44.0 ± 2.4 (8)	6.5 ± 4.5 (5)*†	-40.1 ± 2.9 (8)
Low- K^+ IS w/GABA	No APs (5)*†	No APs (5)*	No APs (5)*†

Abbreviations: ACSF, artificial cerebral spinal fluid; AP, action potential; GABA, γ -amino butyric acid; IS, ischemic solution.

High- K^+ ACSF or 2 mmol/L GABA perfusion prevented AP firing. Data are mean \pm s.e.m. Parentheses indicate n -value. Asterisks (*) indicate significant difference from normoxic controls; daggers (†) indicate significant difference from normoxia at the same time point; and double daggers (‡) indicate significant difference from IS alone. Treatments as per Figure 4.

samples ($n = 3$ for each, Figure 5D), suggesting that the induction of apoptosis in IS-treated cortical sheets at 24 hours is at a very early stage. Finally, we also assayed total cellular [ATP] at 1 and 24 hours and found that [ATP] was unchanged after 1 hour of IS treatment, but decreased $\sim 75\%$ in IS-treated samples at 24 hours ($n = 3$ to 5, Figure 5E). Nonetheless in samples that were treated with IS and then allowed to recover in normoxic ACSF for 1 hour, [ATP] began to recover, suggesting that samples treated with this paradigm remain viable and recover from prolonged IS exposure.

Discussion

We show that in addition to being anoxia-tolerant, Western painted turtle cortical neurons are tolerant to a high- K^+ ischemic penumbral mimic solution. This conclusion is supported by our observations that turtle neurons: (1) depolarize but are electrically quiescent during 1 hour of IS perfusion and recover fully after normoxic reperfusion; (2) defend [ATP] in this time period, and [ATP] recovers from ischemic lows after 24 hours treatment; and (3) maintain plasma membrane and DNA integrity through 24 hours of IS treatment. Although turtles likely do not experience ischemia naturally, this tolerance is nonetheless remarkable and the mechanisms that mediate this survival may be used to protect tissue in ischemia-sensitive mammals. An important component of this tolerance during the transition to IS treatment and reperfusion is an increase in inhibitory GABAergic signaling. GABA is released in anoxic turtle brain (Nilsson and Lutz, 1991) and upon binding to postsynaptic GABA_A receptors, activates G_{Cl} to a degree sufficient to dominate G_w , and thus clamp V_m at E_{GABA} (Pamerter *et al*, 2011). As a result, excitatory inputs are neutralized by a ready flux of opposing charge mediated by Cl^- , which dampens excitatory depolarization via a shunt-like mechanism. Here, we report a similar phenotype in IS-treated cortex: V_m depolarizes to E_{GABA} ; G_w increases >3 -fold and neurons are electrically silent despite extreme depolarization, while APs cannot be elicited with stimulus injection.

The mechanism underlying these postsynaptic changes is likely mediated by GABA receptor activation since (1) GABA perfusion in normoxic ACSF increases neuronal G_w to the same degree as IS and APs cannot be elicited; while (2) cotreatment of IS plus GABA does not result in further elevations of G_w ; and (3) antagonism of neuronal GABA_{A+B} receptors during IS prevents the IS-mediated increase in G_w , and neurons become hyperexcited and V_m runs down within minutes of reperfusion. Therefore, since IS and GABA have similar but not additive effects on G_w and neuronal excitability, and since GABAergic inhibition during IS treatment prevents the increase in G_w and induces excitotoxicity characteristic of ischemic mammalian neurons, we conclude that enhanced GABAergic inhibition prevents electrical excitability and at a minimum, underlies early-stage IS tolerance in this model.

GABAergic inhibition and the large depolarizing shift in E_{GABA} are mediated by the high $[K^+]$ of our IS. In mammals, a high $[K^+]$ perfusate induces extensive neuronal hyperexcitation by shifting the K^+ gradient such that nervous cells depolarize and become more electrically active within 4 to 5 minutes of perfusion (Zhou *et al*, 2010). In mammalian slice models, this excitation leads to depolarization of both presynaptic and postsynaptic neurons, which causes extensive neurotransmitter release, excitotoxicity, and spreading depression (Gardner-Medwin, 1981). Conversely, in turtle brain high- K^+ ACSF causes extensive postsynaptic depolarization, but electrical activity is suppressed and V_m recovers after reperfusion with normal ACSF. GABAergic increases in postsynaptic G_w are activated by high- K^+ and do not occur in neurons treated with low- K^+ IS, indicating that presynaptic GABA release is greatly increased by high- K^+ . Our observation that turtle neurons are electrically silent in high- K^+ experiments despite significant depolarization is notable as this indicates that inhibitory tone in turtle brain greatly outweighs excitatory tone, as in these experiments the high $[K^+]$ will have chronically activated excitatory glutamatergic signaling in addition to inhibitory GABAergic signaling. This may represent a significant adaptive advantage in turtle brain relative to mammal brain. Conversely, our observation that turtle neurons

treated with low- K^+ IS do not exhibit increases in G_w , also indicates that this change is mediated by activation of postsynaptic GABA receptors due to high- K^+ -induced presynaptic GABA release. The lack of electrical hyperexcitability in neurons treated with low- K^+ IS indicates that the remaining deleterious alterations in this solution are not overly damaging to turtle neurons, or are protected against by alternative mechanisms since the inhibitory GABAergic shunt that underlies SA does not appear to be active under these conditions.

In addition to regulating GABA release during IS perfusion, high- K^+ also predominately mediates the depolarizing shift in E_{GABA} observed in IS-treated neurons. E_{GABA} is the reversal potential of GABA_A receptors, which are primarily permeant to Cl^- ions. E_{GABA} therefore is determined by the Cl^- gradient, which is in turn determined by the activity of K^+/Cl^- cotransporters (Rivera *et al*, 1999). Therefore, increasing external K^+ decreases the driving force on Cl^- , and depolarizes E_{GABA} . This relationship is supported by our observations that high- K^+ alone in ACSF was sufficient to depolarize E_{GABA} in normoxia and shift V_m toward this depolarized value, and that low- K^+ IS did not induce a shift in V_m or E_{GABA} , even when postsynaptic GABA_A receptors were chronically activated in the presence of 2 mmol/L GABA. Conversely, in anoxic turtle cortex GABA release is drastically increased, but E_{GABA} is not depolarized and extracellular $[K^+]$ does not change significantly during prolonged anoxia, suggesting that alternative mechanisms are used to activate endogenous inhibitory GABAergic neuroprotective mechanisms in anoxic turtle brain (Jackson and Heisler, 1983; Nilsson and Lutz, 1991; Pamenter *et al*, 2011).

Traditionally researchers have primarily used oxygen-glucose deprivation or chemical ischemia to mimic stroke *in vitro*. Although these paradigms accurately model the metabolic consequence of impaired cerebral blood flow, they do not incorporate other deleterious aspects of the ischemic milieu (Lo, 2008; Yao *et al*, 2007). The ischemic paradigm used in our experiments similarly mimics the metabolic consequences of reduced cerebral blood flow (low glucose, hypoxia), but also incorporates severe ionic derangements, acidification (\sim pH 6.4), and excitatory neurotransmitter accumulation (glutamate) characteristic of ischemic mammalian penumbral tissue (Hansen and Nedergaard, 1988; Siesjo, 1992; Yao *et al*, 2007). Indeed, many of these alterations alone are sufficient to induce depolarization or death in mammalian neurons. For example, the increase in external $[K^+]$ from 2.6 (in ACSF) to 64 mmol/L (in IS) is sufficient to induce spreading depression in cortex (Zhou *et al*, 2010), whereas holding external pH at 6.4 for 6 hours causes 50% neuronal and glial cell mortality in forebrain (Nedergaard *et al*, 1991). Therefore when combined, these alterations present a highly challenging stress, and the ability of turtle cortex to withstand IS treatment for up to 24 hours with minimal apparent damage is remarkable.

Unlike turtle neurons, mammalian cells are intolerant to IS treatment. In hippocampal slice models and in cell cultures, mammalian neurons become electrically excited and rapidly depolarize within minutes of IS onset at 24°C or 37°C, and V_m does not recover after normoxic reperfusion (Yao and Haddad, unpublished observations). Furthermore, after a 24-hour IS treatment \sim 90% of neurons take up PI and $>$ 90% of cellular lactate dehydrogenase is released (Yao *et al*, 2007), while [ATP] is depleted $>$ 85%, and DNA exhibits extensive oligonucleosomal fragmentation and TUNEL (terminal deoxynucleotidyl transferase-mediated 2'-deoxyuridine 5'-triphosphate-biotin nick end labeling)-positive staining characteristic of late-stage apoptosis (Galluzzi *et al*, 2007; Pamenter *et al*, 2010, 2012). Similar results have been reported in a wide variety of *in vivo* and *in vitro* models of the ischemic mammalian penumbra, where in general ischemic stress induces: electrical hyperexcitation and extreme V_m depolarization within minutes; ionic and neurotransmitter derangements, [ATP] depletion, and necrotic cell rupture or extensive activation of apoptotic mechanisms within $<$ 1 to 4 hours; and extensive or total neuronal cell death within 6 to 24 hours (Broughton *et al*, 2009; Hansen and Nedergaard, 1988; Nedergaard and Hansen, 1993; Siesjo, 1992).

Comparatively, patch-clamped turtle cortical neurons tolerate at least 60 minutes of IS treatment (i.e., at least 20 to 30 \times longer than mammalian neurons) and V_m and synaptic function fully recover after reperfusion. Necrosis does not occur through 24 hours of IS treatment, as indicated by maintained vital dye exclusion, and DNA does not exhibit fragmentation typical of either necrosis or apoptotic cell degradation at 24 hours (Galluzzi *et al*, 2007). However, we observed a significant increase in the translocation of annexin V, an early indicator of apoptosis (Galluzzi *et al*, 2007), after 24 hours, but not 4 hours of IS treatment. This result suggests that cortical sheets are likely reaching the limit of their tolerance to the stress at this point and are beginning to undergo programmed cell death. Nonetheless, the recovery of [ATP] after 1-hour reperfusion after 24 hours IS treatment suggests that tissue remains viable and recovers even after prolonged stress. There is evidence that cells damaged by ischemic stress are replaced via neuronal regeneration in this model (Kesaraju and Milton, 2009), and it is tempting to speculate that *in vivo*, damaged cells marked for apoptosis would be replaced by new neurons, potentially allowing this organism to tolerate prolonged brain ischemia and recover without long-term detriment, even if some cells are damaged by the initial stress. If this were the case, then the observed annexin V staining at 24 hours may actually be adaptive in turtle brain and indicative of maintenance-related local apoptosis to mark damaged cells for removal and eventual replacement with new neurons, instead of an indication of the onset of widespread apoptosis.

Experimental temperature differences may contribute to the enhanced ischemia tolerance of turtle brain in the present study relative to previously published studies in mammal brain. Mammalian experiments are typically conducted between 24°C and 37°C, and hypothermia slows metabolism and extends ischemic or hypoxic survival time (Lampe and Becker, 2011). Conversely, turtles survive months of anoxia at 4°C, and typically tolerate 2 to 3 days of anoxia at room temperature, and just hours at 37°C (Bickler and Buck, 2007). Nonetheless, turtles have consistently displayed a remarkable degree of anoxia and ischemia tolerance relative to mammals across a wide range of experimental temperatures (Belkin, 1968; Bickler, 1992; Bickler and Buck, 2007; Doll *et al*, 1991) and our present results provide further support for this relationship. For example, at temperatures of 22°C to 24°C turtle brain sheets tolerate >3 hours of anoxic perfusion and >1 hour of ischemic perfusion, whereas rat brain slices last <40 minutes in anoxia and <5 minutes in ischemia (Doll *et al*, 1991; Pamerter *et al*, 2010, present study). Similarly at the whole-organism level, turtles tolerate >1 hour of ischemia after cardiac excision, while mammals die within minutes of blood flow cessation (Belkin, 1968; Bickler and Buck, 2007).

In summary, we have shown that turtle cortical neurons tolerate a highly deleterious ischemic stress for up to 24 hours. Electrophysiological studies indicate that one key mechanism underlying this tolerance is a large-scale activation of inhibitory GABAergic G_{Cl} , which clamps V_m at E_{GABA} and prevents excitatory events and cell death during IS onset. A similar mechanism underlies spike arrest in the anoxic turtle cortex, but the degree to which inhibitory GABAergic mechanisms are activated in IS-treated neurons is several-fold greater than that observed previously in anoxic experiments (Pamerter *et al*, 2011), likely because GABAergic inhibition here is activated by greatly increased extracellular K^+ , whereas in the anoxic cortex GABA release is activated by an unknown mechanism that is likely K^+ independent. Nonetheless, these results illustrate that naturally evolved adaptations to survival in anoxic environments can also protect against clinically relevant paradigms of ischemic stress derived from mammalian studies. This study highlights the value of a comparative model in which to elucidate medically relevant protective mechanisms against anoxic and ischemic insults in brain.

Acknowledgements

The authors graciously thank Ms Jennifer Meerloo and Mrs Orit Gavrialov for expert technical assistance.

Disclosure/conflict of interest

The authors declare no conflict of interest.

References

- Anderson RE, Tan WK, Martin HS, Meyer FB (1999) Effects of glucose and PaO₂ modulation on cortical intracellular acidosis, NADH redox state, and infarction in the ischemic penumbra. *Stroke* 30:160–70
- Arundine M, Tymianski M (2004) Molecular mechanisms of glutamate-dependent neurodegeneration in ischemia and traumatic brain injury. *Cell Mol Life Sci* 61:657–68
- Attwell D, Laughlin SB (2001) An energy budget for signaling in the grey matter of the brain. *J Cereb Blood Flow Metab* 21:1133–45
- Belkin DA (1968) Anaerobic brain function: effects of stagnant and anoxic anoxia on persistence of breathing in reptiles. *Science* 162:1017–8
- Bickler PE (1992) Effects of temperature and anoxia on regional cerebral blood flow in turtles. *Am J Physiol* 262:R538–41
- Bickler PE, Buck LT (2007) Hypoxia tolerance in reptiles, amphibians, and fishes: life with variable oxygen availability. *Annu Rev Physiol* 69:145–70
- Bickler PE, Donohoe PH, Buck LT (2000) Hypoxia-induced silencing of NMDA receptors in turtle neurons. *J Neurosci* 20:3522–8
- Blanton MG, Lo Turco JJ, Kriegstein AR (1989) Whole cell recording from neurons in slices of reptilian and mammalian cerebral cortex. *J Neurosci Methods* 30:203–10
- Branston NM, Symon L, Crockard HA, Pasztor E (1974) Relationship between the cortical evoked potential and local cortical blood flow following acute middle cerebral artery occlusion in the baboon. *Exp Neurol* 45:195–208
- Broughton BR, Reutens DC, Sobey CG (2009) Apoptotic mechanisms after cerebral ischemia. *Stroke* 40:e331–9
- Buck L, Espanol M, Litt L, Bickler P (1998) Reversible decreases in ATP and PCR concentrations in anoxic turtle brain. *Comp Biochem Physiol A Mol Integr Physiol* 120:633–9
- Costa C, Leone G, Saule E, Pisani F, Bernardi G, Calabresi P (2004) Coactivation of GABA(A) and GABA(B) receptor results in neuroprotection during *in vitro* ischemia. *Stroke* 35:596–600
- Doll CJ, Hochachka PW, Reiner PB (1991) Effects of anoxia and metabolic arrest on turtle and rat cortical neurons. *Am J Physiol Regul Integr Comp Physiol* 260:R747–55
- Erecinska M, Silver IA (1989) ATP and brain function. *J Cereb Blood Flow Metab* 9:2–19
- Feng ZC, Rosenthal M, Sick TJ (1988) Suppression of evoked potentials with continued ion transport during anoxia in turtle brain. *Am J Physiol* 255:R478–84
- Galluzzi L, Maiuri MC, Vitale I, Zischka H, Castedo M, Zitvogel L, Kroemer G (2007) Cell death modalities: classification and pathophysiological implications. *Cell Death Differ* 14:1237–43
- Gardner-Medwin AR (1981) Possible roles of vertebrate neuroglia in potassium dynamics, spreading depression and migraine. *J Exp Biol* 95:111–27
- Hansen AJ (1985) Effect of anoxia on ion distribution in the brain. *Physiol Rev* 65:101–48
- Hansen AJ, Nedergaard M (1988) Brain ion homeostasis in cerebral ischemia. *Neurochem Pathol* 9:195–209
- Hochachka PW (1986) Defense strategies against hypoxia and hypothermia. *Science* 231:234–41
- Hodgkin AL, Huxley AF (1952) A quantitative description of membrane current and its application to conduction and excitation in nerve. *J Physiol* 117:500–44

- Hylland P, Milton S, Pek M, Nilsson GE, Lutz PL (1997) Brain Na⁺/K⁺-ATPase activity in two anoxia tolerant vertebrates: crucian carp and freshwater turtle. *Neurosci Lett* 235:89–92
- Jackson DC, Heisler N (1983) Intracellular and extracellular acid-base and electrolyte status of submerged anoxic turtles at 3C. *Respir Physiol* 53:187–201
- Kesaraju S, Milton SL (2009) Preliminary evidence of neuronal regeneration in the anoxia tolerant vertebrate brain. *Exp Neurol* 215:401–3
- Krnjevic K (1997) Role of GABA in cerebral cortex. *Can J Physiol Pharmacol* 75:439–51
- Lampe JW, Becker LB (2011) State of the art in therapeutic hypothermia. *Annu Rev Med* 62:79–93
- Lo EH (2008) A new penumbra: transitioning from injury into repair after stroke. *Nat Med* 14:497–500
- Nedergaard M, Goldman SA, Desai S, Pulsinelli WA (1991) Acid-induced death in neurons and glia. *J Neurosci* 11:2489–97
- Nedergaard M, Hansen AJ (1993) Characterization of cortical depolarizations evoked in focal cerebral ischemia. *J Cereb Blood Flow Metab* 13:568–74
- Nilsson GE, Lutz PL (1991) Release of inhibitory neurotransmitters in response to anoxia in turtle brain. *Am J Physiol* 261:R32–7
- Pamerter ME, Ali SS, Tang Q, Finley JC, Gu XQ, Dugan LL, Haddad GG (2012) An *in vitro* ischemic penumbral mimic perfusate increases NADPH oxidase-mediated superoxide production in cultured hippocampal neurons. *Brain Res* 1452:165–72
- Pamerter ME, Buck LT (2008) delta-Opioid receptor antagonism induces NMDA receptor-dependent excitotoxicity in anoxic turtle cortex. *J Exp Biol* 211:3512–7
- Pamerter ME, Hogg DW, Ormond J, Shin DS, Woodin MA, Buck LT (2011) Endogenous GABA(A) and GABA(B) receptor-mediated electrical suppression is critical to neuronal anoxia tolerance. *Proc Natl Acad Sci USA* 108:11274–9
- Pamerter ME, Shin DS, Buck LT (2008) AMPA receptors undergo channel arrest in the anoxic turtle cortex. *Am J Physiol Regul Integr Comp Physiol* 294:R606–13
- Pamerter ME, Tjong J, Perkins G, Meerloo J, Ryu J, Gu X, Ellisman M, Haddad GG (2010) An *in vitro* ischemic penumbral mimic solution induces autophagic cell death in hippocampal neuronal or type-I astrocytic cultures. In: *2010 Neuroscience Meeting Planner* Vol. 1452. San Diego: Society for Neuroscience, pp 165–72
- Rivera C, Voipio J, Payne JA, Ruusuvuori E, Lahtinen H, Lamsa K, Pirvola U, Saarma M, Kaila K (1999) The K⁺/Cl⁻ co-transporter KCC2 renders GABA hyperpolarizing during neuronal maturation. *Nature* 397:251–5
- Siesjo BK (1992) Pathophysiology and treatment of focal cerebral ischemia. Part I: Pathophysiology. *J Neurosurg* 77:169–84
- Thompson SM, Gahwiler BH (1989) Activity-dependent disinhibition. II. Effects of extracellular potassium, furosemide, and membrane potential on ECl⁻ in hippocampal CA3 neurons. *J Neurophysiol* 61:512–23
- Wasser JS, Warburton SJ, Jackson DC (1991) Extracellular and intracellular acid-base effects of submergence anoxia and nitrogen breathing in turtles. *Respir Physiol* 83:239–52
- Yao H, Shu Y, Wang J, Brinkman BC, Haddad GG (2007) Factors influencing cell fate in the infarct rim. *J Neurochem* 100:1224–33
- Zhou N, Gordon GR, Feighan D, MacVicar BA (2010) Transient swelling, acidification, and mitochondrial depolarization occurs in neurons but not astrocytes during spreading depression. *Cereb Cortex* 20:2614–24

Supplementary Information accompanies the paper on the Journal of Cerebral Blood Flow & Metabolism website (<http://www.nature.com/jcbfm>)